

# Correction to “Determination of Chain Flip Rates in Poly(ethylene) Crystallites by Solid-State Low-Field $^1\text{H}$ NMR for Two Different Sample Morphologies”

R. Bärenwald, Y. Champouret, K. Saalwächter,\* and K. Schäler\*

*J. Phys. Chem. B* **2012**, *116* (43), 13089–13097. DOI: 10.1021/jp3061625

In our previous publication,<sup>1</sup> we used a log-normal distribution of correlation times

$$p(\ln \tau_c, \mu, \sigma) = \frac{1}{\sqrt{2\pi}\sigma} \exp\left\{-\frac{(\ln \tau_c - \mu)^2}{2\sigma^2}\right\} \quad (1)$$

where

$$\mu = \langle \ln \tau_c \rangle \quad (2)$$

to describe the monomer jump motion within poly(ethylene) crystallites. This local process mediates the well-known, mechanically active large-scale intracrystalline chain transport. We performed  $^1\text{H}$  NMR magic-sandwich echo decay experiments for the crystalline signal as obtained by decomposition of the free-induction decay (FID) and fitted the data taken as a function of pulse sequence time  $t_{\text{seq}}$  via a numerical integral over eq 1 multiplied by a theoretical expression  $S_{\text{MSE}}(t_{\text{seq}}, \Delta M_2^{\text{dyn}}, \tau_c)$

$$S_{\text{MSE}}^{\text{distr}} = \int_0^\infty p(\ln \tau_c, \mu, \sigma) S_{\text{MSE}}(t_{\text{seq}}, \Delta M_2^{\text{dyn}}, \tau_c) d \ln \tau_c \quad (3)$$

Equations 1 and 3 correct eqs 6 and 7 of our paper in that an integration on an  $\ln \tau_c$  scale is strongly advised. Our implementation of the corresponding integral (linear in  $\tau_c$  but with increasing interval length in order to cover large  $\tau_c$ ) was subject to numerical inaccuracies related to the upper  $\tau_c$  limit. Here, we correct the associated, in fact not too large, errors, implementing the integral by a summation over 50 values of  $\ln \tau_c$  ranging from  $-3$  to  $3$  standard deviations  $\sigma$ . The latter roughly corresponds to the overall distribution width in decades.

Much more importantly, we have relied upon a mathematically correct but physically unreasonable quantity for the average correlation time, i.e., the arithmetic average (mean) of the log-normal distribution on a linear  $\tau_c$  scale,  $\langle \tau_c \rangle = \exp\{\mu + \sigma^2/2\}$ . This value is highly unsuitable, as it is heavily biased toward the high- $\tau_c$  end of the distribution if  $\sigma$  is significantly larger than 1, corresponding to  $>1$  decade wide distributions. A more feasible average is taken on a logarithmic scale

$$\bar{\tau}_c = \exp\{\langle \ln \tau_c \rangle\} = \exp\{\mu\} \quad (4)$$

which corresponds to the *median* of the distribution rather than the mean and corrects eq 8 of the paper. This suitable definition of an average has been common practice in several, but certainly not all, NMR studies of polymers<sup>2</sup> or small molecules<sup>3,4</sup> approaching the glass transition, where wide distributions are common. It better reflects the behavior of the majority of ensemble members.

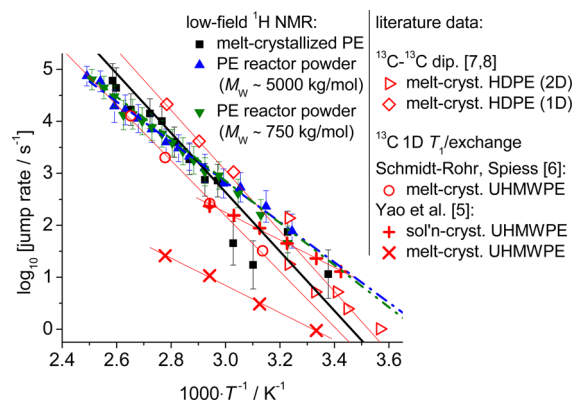


**Figure 1.** Corrected Arrhenius plot of the jump rates  $\bar{k} = 1/(2\bar{\tau}_c)$  for the different PE samples in comparison with literature data. The thick lines visualize the results from the variable-temperature fitting.

Our second and more reliable approach to data treatment consisted of simultaneous fitting of temperature-dependent data, which is implemented by combination of eq 3 with the Arrhenius law

$$\mu(T) = \ln \tau_c^0 + \frac{E_a}{RT} \quad (5)$$

The overall fitting quality of raw data by the two approaches, Figures 6 and 9 of the paper, respectively, does not change visibly, so we refrain from showing updated plots. Some of the fitted parameters, however, change appreciably, so Figure 1 and Table 1 show corrected versions of Figure 8 and Table 1 of the paper, respectively. In Figure 1, we now also include lines corresponding to the activation parameters obtained from fitting data at variable  $T$  (second approach), which were only listed in the table and not visualized in the paper. They provide a better comparison of the two approaches than just the tabulated values.

We observe that the major conclusions of the paper do not change, mainly because the distribution widths  $\sigma$  found for most samples are not too different, varying between about 1 and 1.5 decades. Nevertheless, the results now demonstrate that the reactor powder samples show, in the lower temperature range, a trend toward somewhat faster monomer flips in the crystallites. This is in fact more in line with the previous observations by Yao et al.,<sup>5</sup> who observed significantly (a factor  $>10$ ) faster long-range intracrystalline chain diffusion in an adjacent-reentry dominated solution-grown UHMWPE sample

Published: October 20, 2014

Table 1. Corrected Comparison of Results from Different Methods of Data Analysis

	melt-cryst. PE	PE reactor powder, $M_w \sim 750$ kg/mol	PE reactor powder, $M_w \sim 5000$ kg/mol
		Analysis of $I_c(t_{\text{seq}}) _{T=\text{const}}$	
$\Delta M_2^{\text{dyn}}$ (kHz <sup>2</sup> )	6700	6700 $\pm$ 800	6700
$\sigma$ (kHz <sup>2</sup> )	1.57	1.57 $\pm$ 0.23	1.57
$E_a$ (kJ·mol <sup>-1</sup> )	97 $\pm$ 45	80 $\pm$ 17	73 $\pm$ 19
$\log[\tau_c^0(\text{s})]$	-18.1 $\pm$ 6.4	-15.5 $\pm$ 2.3	-14.5 $\pm$ 2.8
		Analysis of $I_c(T) _{t_{\text{eq}}=\text{const}}$	
$\Delta M_2^{\text{dyn}}$ (kHz <sup>2</sup> )	5720 $\pm$ 590	6010 $\pm$ 360	6610 $\pm$ 430
$\sigma$ (kHz <sup>2</sup> )	1.13 $\pm$ 0.22	1.31 $\pm$ 0.10	1.51 $\pm$ 0.10
$E_a$ (kJ·mol <sup>-1</sup> )	114 $\pm$ 7	77.5 $\pm$ 2.2	73.5 $\pm$ 2.2
$\log[\tau_c^0(\text{s})]$	-20.7 $\pm$ 1.0	-15.32 $\pm$ 0.32	-14.73 $\pm$ 0.32

as compared to a melt-crystallized counterpart. The reactor powders are likely less ideal and therefore do not exhibit a correspondingly accelerated jump process. We note, however, that the comparison with literature data in Figure 1 reveals that it is the melt-crystallized sample of Yao et al. which deviates significantly downward from all other shown literature examples of melt-crystallized (UHMW)PE samples.<sup>6–8</sup>

## REFERENCES

- (1) Bärenwald, R.; Champouret, Y.; Saalwächter, K.; Schäler, K. Determination of Chain Flip Rates in Poly(ethylene) Crystallites by Solid-State Low-Field <sup>1</sup>H NMR for Two Different Sample Morphologies. *J. Phys. Chem. B* **2012**, *116*, 13089–13097.
- (2) Schaefer, D.; Spiess, H. W. Two-dimensional Exchange Nuclear Magnetic Resonance of Powder Samples. IV. Distribution of Correlation Times and Line Shapes in the Intermediate Dynamic Range. *J. Chem. Phys.* **1992**, *97*, 7944–7954.
- (3) Vogel, M.; Brinkmann, C.; Eckert, H.; Heuer, A. Silver Dynamics In silver Iodide/Silver Phosphate Glasses Studied by Multi-Dimensional <sup>109</sup>Ag NMR. *Phys. Chem. Chem. Phys.* **2002**, *4*, 3237–3245.
- (4) Sauer, D.; Schuster, B.; Rosenstihl, M.; Schneider, S.; Talluto, V.; Walther, T.; Blochowicz, T.; Stün, B.; Vogel, M. Dynamics of Water-Alcohol Mixtures: Insights from Nuclear Magnetic Resonance, Broadband Dielectric Spectroscopy, and Triplet Solvation Dynamics. *J. Chem. Phys.* **2014**, *140*, 114503.
- (5) Yao, Y. F.; Graf, R.; Spiess, H. W.; Lippits, D. R.; Rastogi, S. Morphological Differences in Semicrystalline Polymers: Implications for Local Dynamics and Chain Diffusion. *Phys. Rev. E* **2007**, *76*, 060801(R).
- (6) Schmidt-Rohr, K.; Spiess, H. W. Chain Diffusion between Crystalline and Amorphous Regions in Polyethylene Detected by 2D Exchange <sup>13</sup>C NMR. *Macromolecules* **1991**, *24*, 5288–5293.
- (7) Hu, W.-G.; Boeffel, C.; Schmidt-Rohr, K. Chain Flips in Polyethylene Crystallites and Fibers Characterized by Dipolar <sup>13</sup>C NMR. *Macromolecules* **1999**, *32*, 1611–1619.
- (8) Hu, W.-G.; Boeffel, C.; Schmidt-Rohr, K. Chain Flips in Polyethylene Crystallites and Fibers Characterized by Dipolar <sup>13</sup>C NMR (Correction). *Macromolecules* **1999**, *32*, 1714.